



UNIVERSIDAD AUTÓNOMA
DE SAN LUIS POTOSÍ

FLANK COLLAPSE AND NEW RELATIVE INSTABILITY ANALYSIS TECHNIQUES APPLIED TO VOLCAN DE COLIMA AND MT ST. HELENS

*Lorenzo Borselli** ,
*Damiano Sarocchi **



Instituto de Geología

*Instituto de Geología

Universidad Autónoma de San Luis Potosí

Av. M. Nava No 5, Zona Universitaria,

San Luis Potosí, 78240, Mexico

lborselli@gmail.com <http://www.lorenzo-borselli.eu>

Colima Volcano - 2011



Mt. St. Helens - 1979



Volcanoes flank collapse

The 1980 sector collapse and debris avalanche at Mount St. Helens triggered the recognition of many similar debris avalanche deposits worldwide (Siebert, 1984; Ui and Glicken, 1986; Siebert et al., 1987; Francis and Wells, 1988; Vallance et al., 1995).

Since then, several studies have revealed that many volcanoes are susceptible to failure caused by exogenous or endogenous processes (McGuire, 1996),



NASA Earth Observatory Image 2009



Volcanoes flank collapse : causes and triggers

Instability of a volcanic edifice may be caused by many factors :

- direct magmatic intrusion into the edifice (Bezymianny-type activity, Gorshkov, 1962 Day, 1996; Elsworth and Voight, 1996),
- deposition of voluminous pyroclastic deposits on steep slopes (McGuire, 1996),
- hydromagmatic processes (Dzurisin, 1998),
- phreatomagmatic activity (Bandai-type activity, Moriya, 1980).
- faulting and tectonic settings (McGuire, 1996; Siebert, 1984)
- Earthquake (Keefer,1984)

Gravitational failures may occur in response to progressive weakening of an edifice. Other triggering mechanisms include phreatic explosions and Hurricane-induced rainfall trigger (flank collapse at the Casita volcano in Nicaragua in 1998, Sheridan et al., 1999; Scott et al., 2005).



A **recently developed technique** of analysis applied to stratovolcanoes by Borselli et al. (2011)*, offers **new insights for assessment of degree of instability for flank collapse of volcanic edifices.**

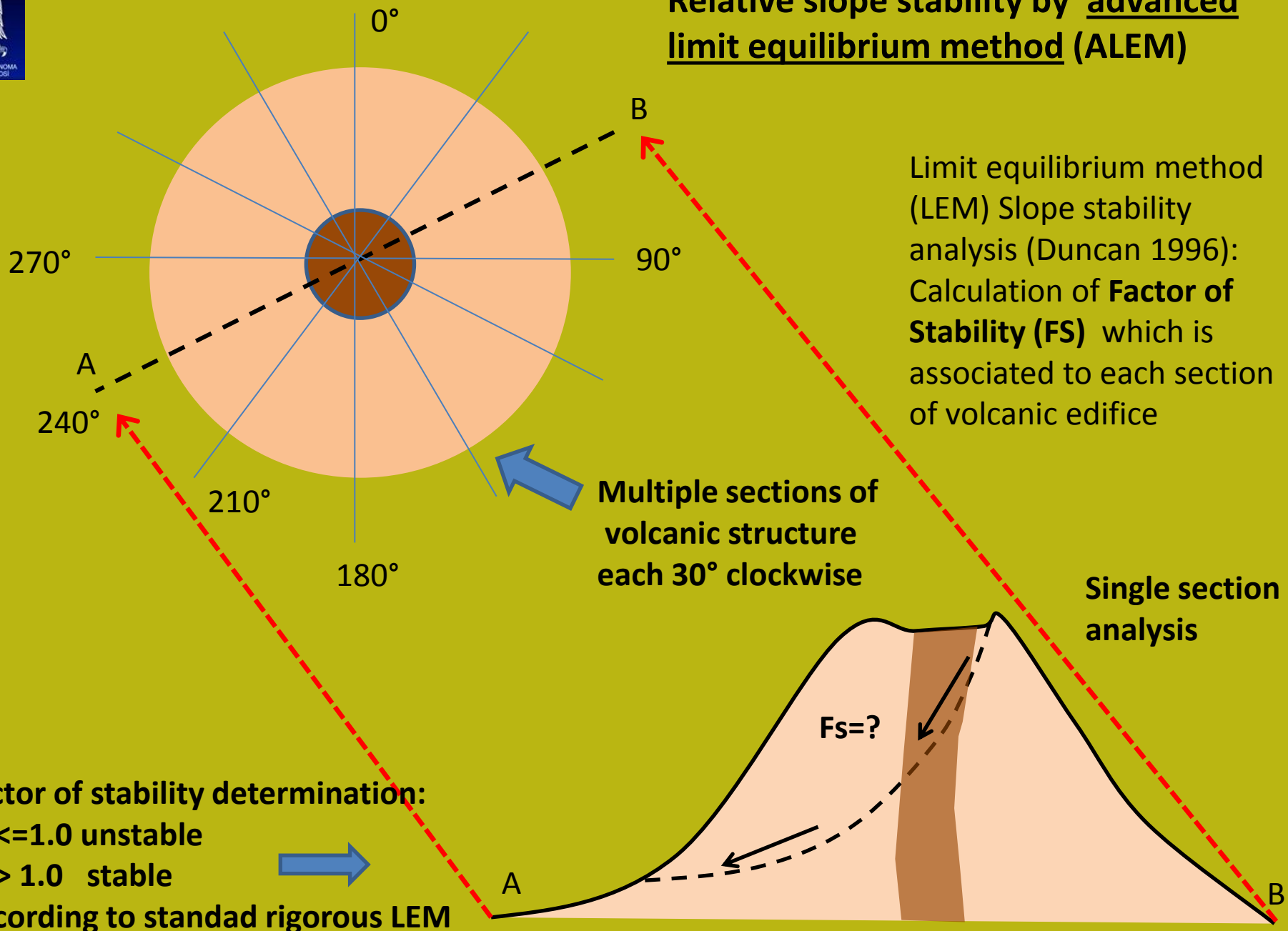
**BORSELLI L., CAPRA L., SAROCCHI D., De La CRUZ-REYNA S. (2011). Flank collapse scenarios at Volcán de Colima, Mexico: a relative instability analysis. Journal of Volcanology and Geothermal Research. 208:51–65.*

The new technique combines three methodologies:

- 1) **slope stability by limit advanced equilibrium analysis (ALEM) of multiple sectors on the volcano** using **SSAP 4.0 (Slope Stability Analysis Software, Borselli 2011)** which include fluid internal overpressure or progressive dissipation (Borselli et al. 2011), and rock mass strength criteria (Hoek et al. 2002,2006) for local, stress state dependent, shear strength;
- 2) the analysis of **relative mass/volume deficit in the volcano structure**, made using the new **VOLCANOFIT 2.0** software (Borselli et al.2011);
- 3) **Statistical analysis of major flank debris avalanche ages in the last 10,000 BP**, using **stochastic arithmetic methods** (Vignes, 1993), and calculating the mean time of recurrence of them.



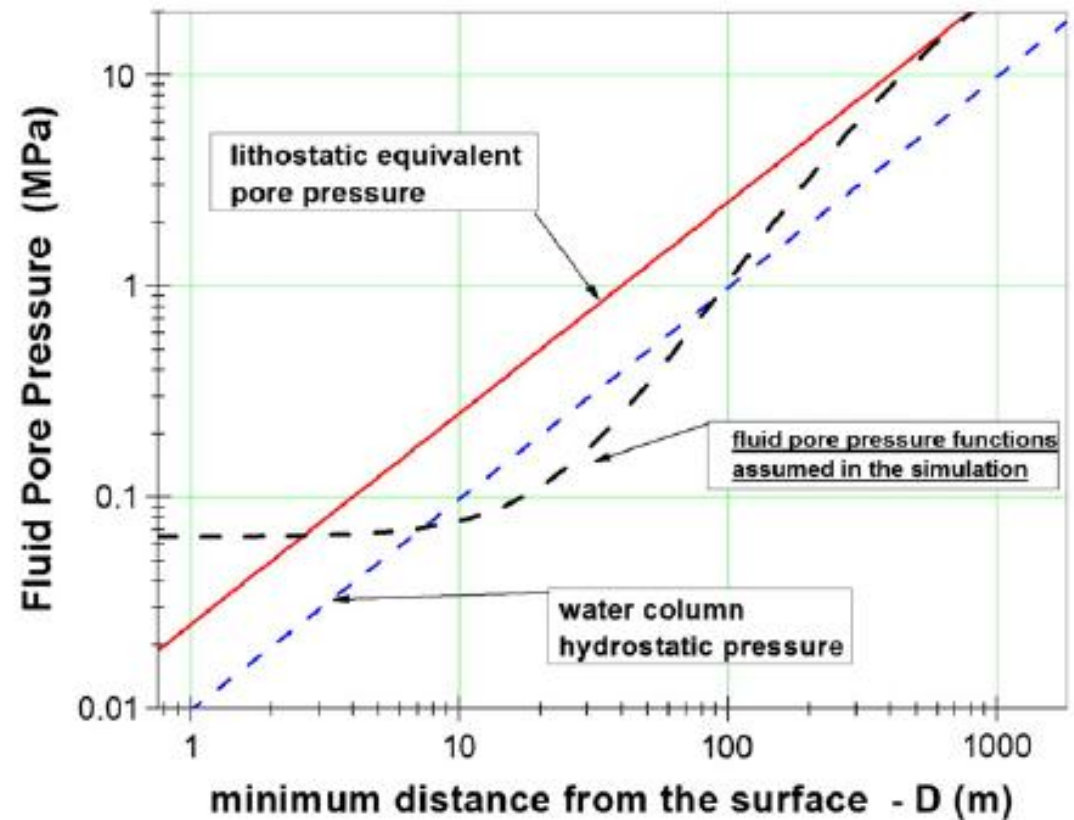
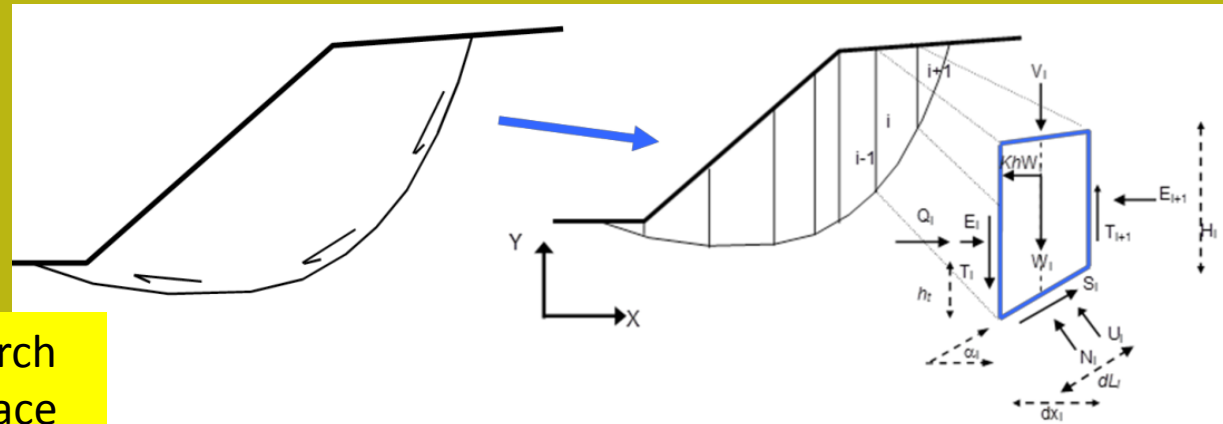
Relative slope stability by advanced limit equilibrium method (ALEM)



SSAP 4.0 is a full freeware software

<http://www.ssap2005.it>
(Borselli 1991, 2011)

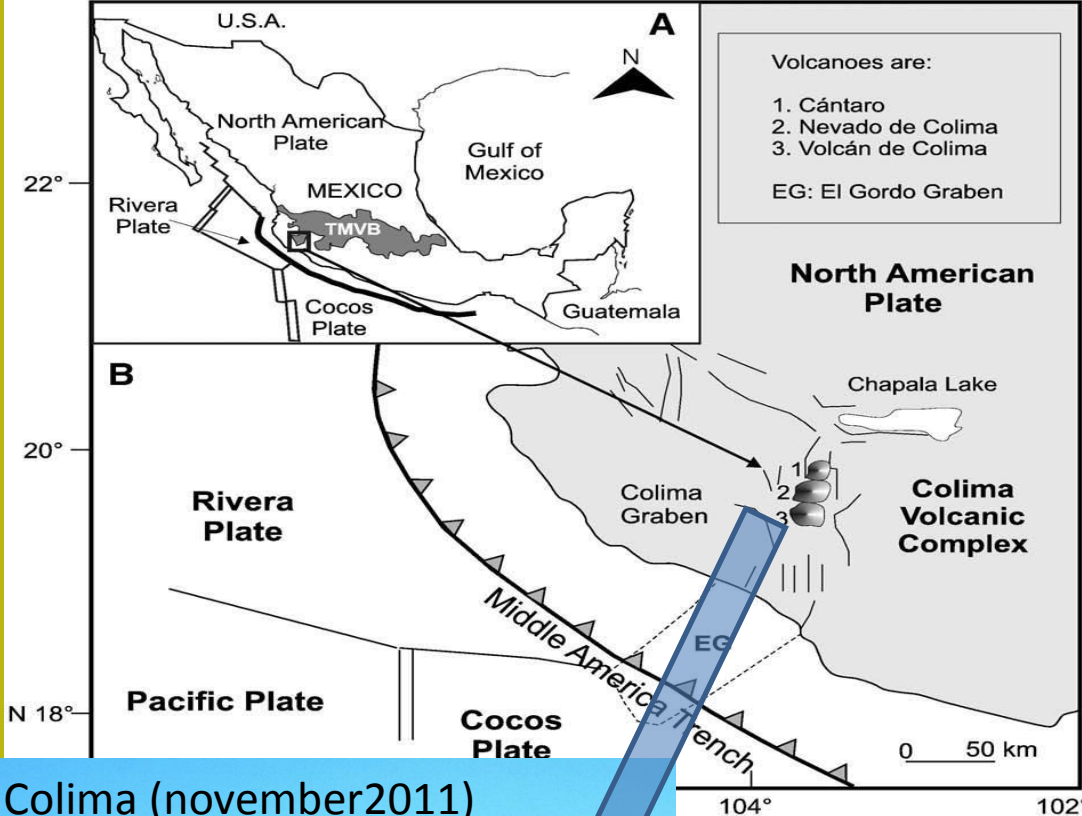
- Generic shape random search of minimum FS sliding surface by Monte Carlo method
- Rock mass strength criterion (Hoek et al. 2002,2006).
- Fluid pressure function (overpressure and dissipation fields Inside volcanic edifice) (Borselli et al. 2011)



$$\sigma_f = \gamma_w z F_D + U_{0_{MIN}}$$

$$F_D = 1 - Ae^{-kD}$$





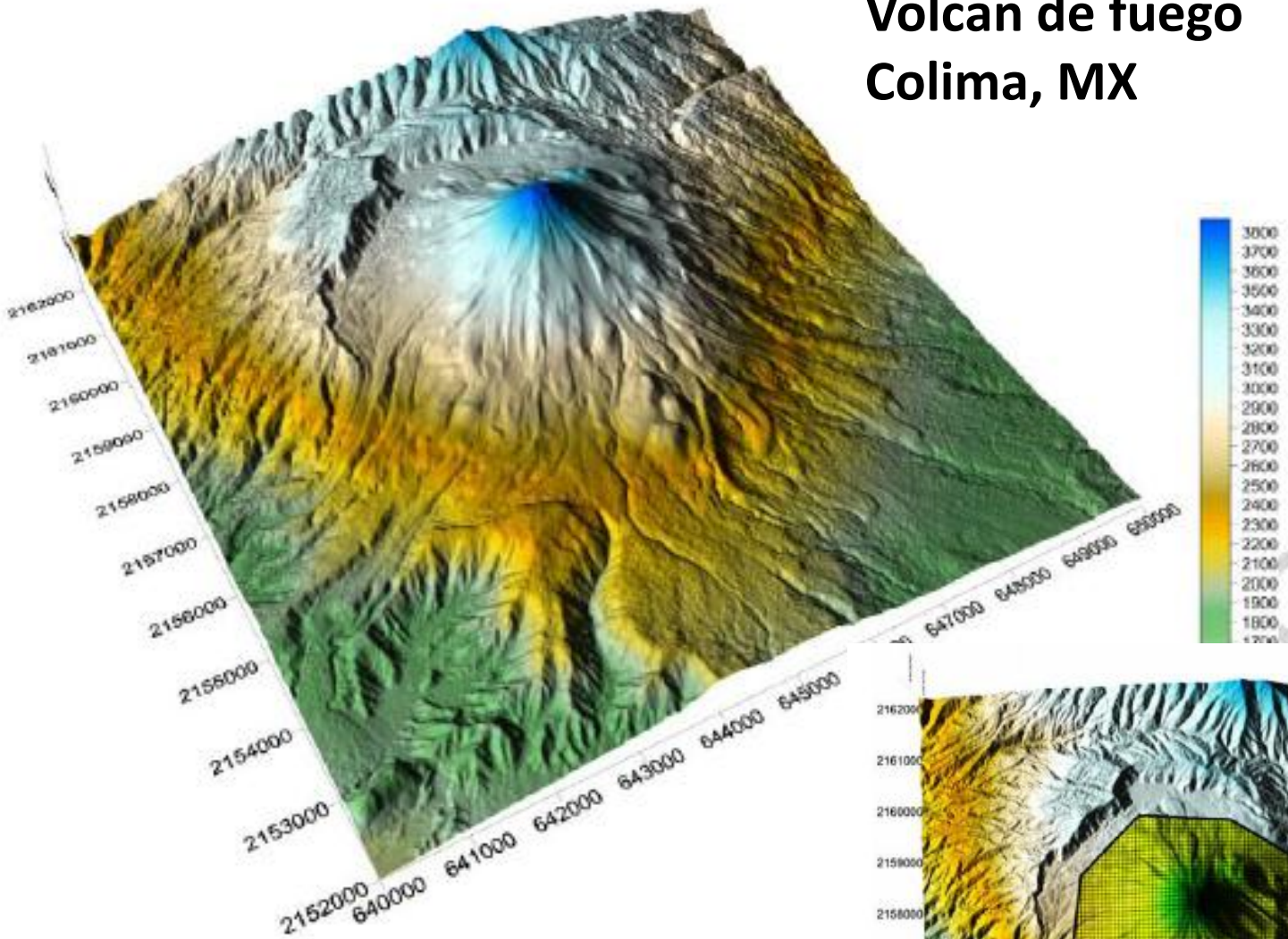
Saucedo et al. 2010

Volcan de Fuego, Colima (november2011)
W view

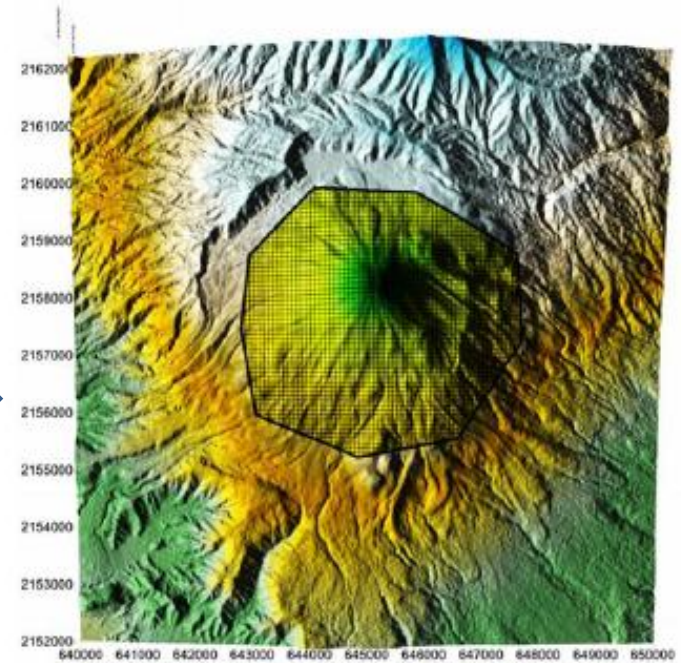


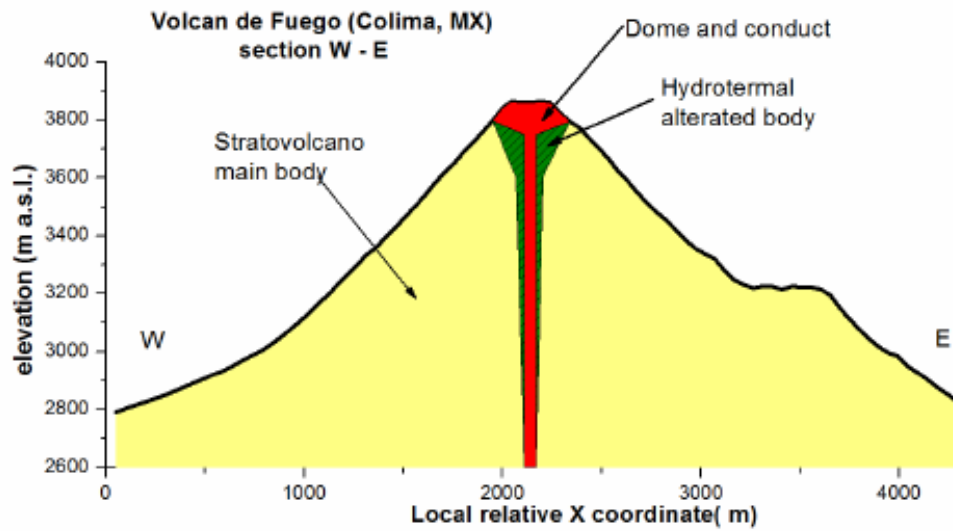
**ALEM analysis application to
Volcan de Fuego, Colima, MX
(Approx 3880 m a.s.l.)**

Volcan de fuego Colima, MX

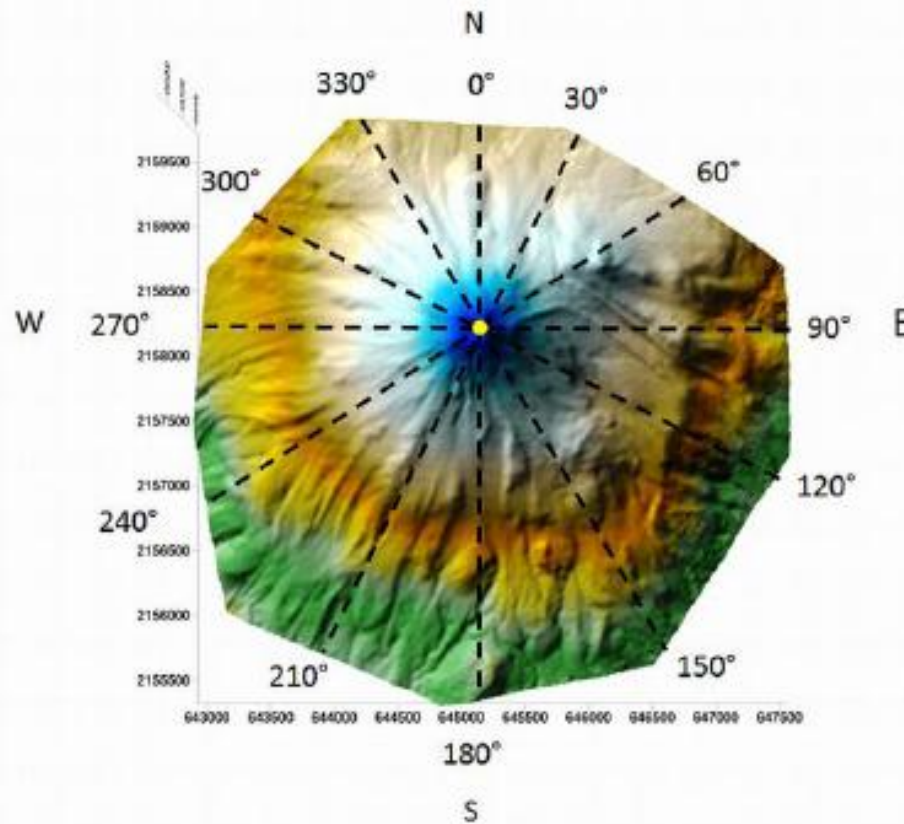
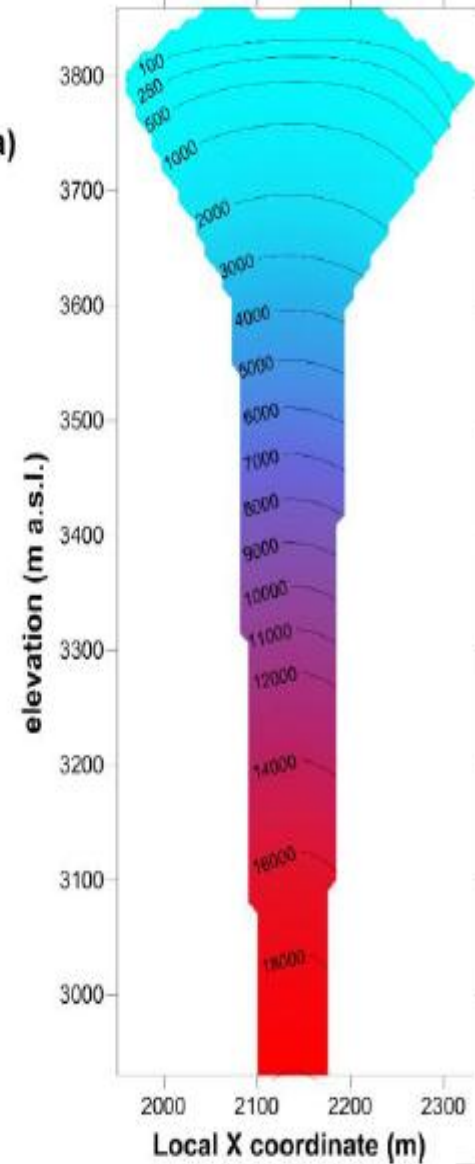
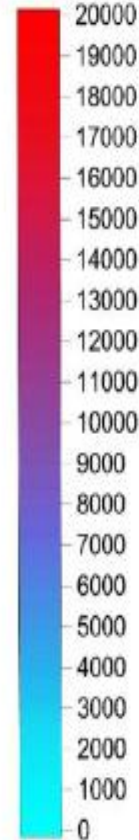


Selected area for analysis





Fluid pressure (kPa)



The advanced Limit equilibrium method (ALEM) and Relative instability analysis Scenarios and mechanical parameters

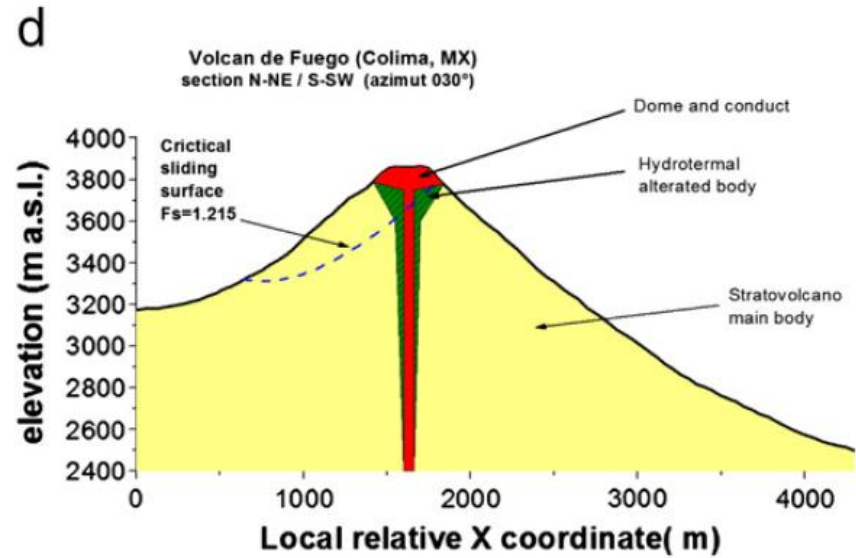
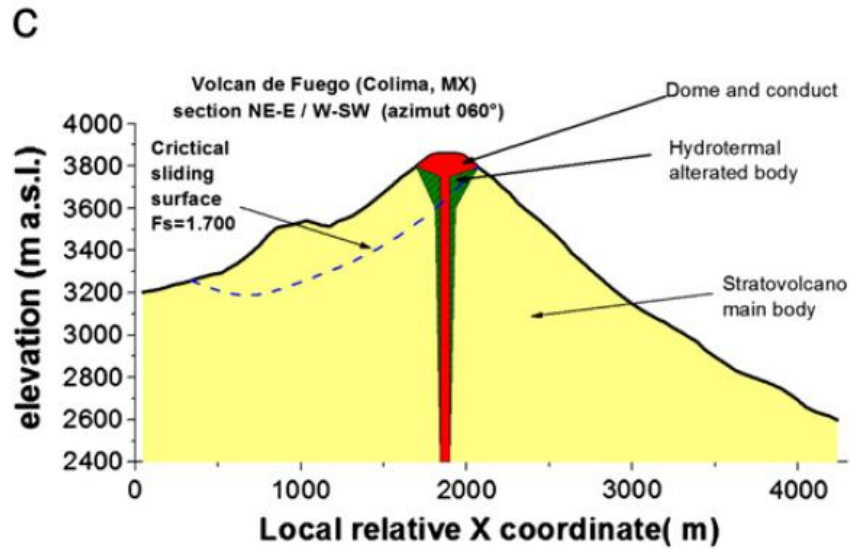
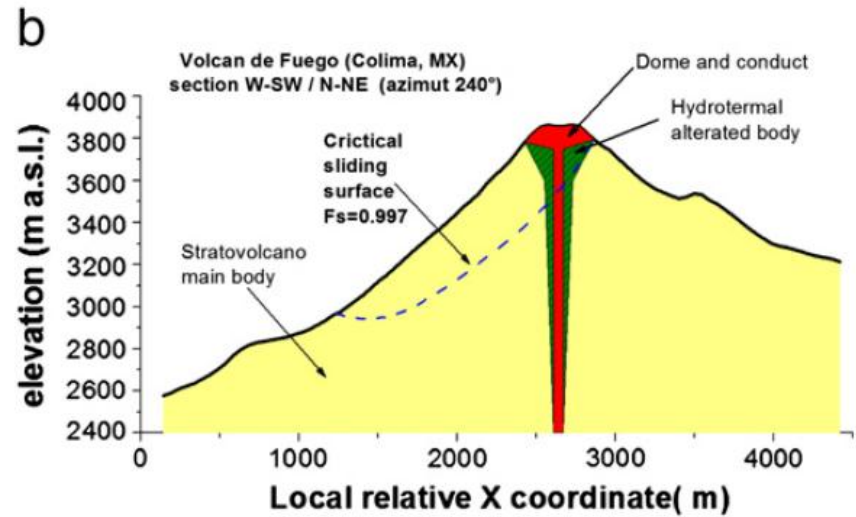
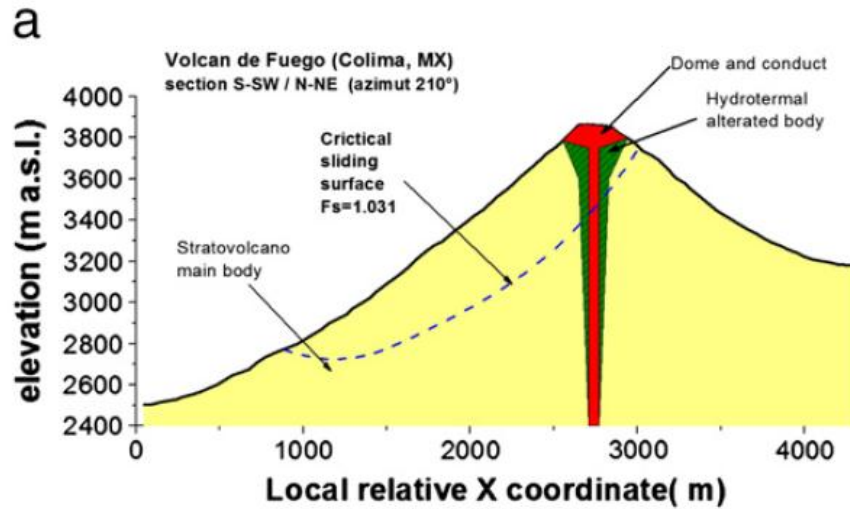
Shear strength parameterization of main bodies of the stratovolcano following the Hoek and Brown strength criterion (Hoek et al., 2002).

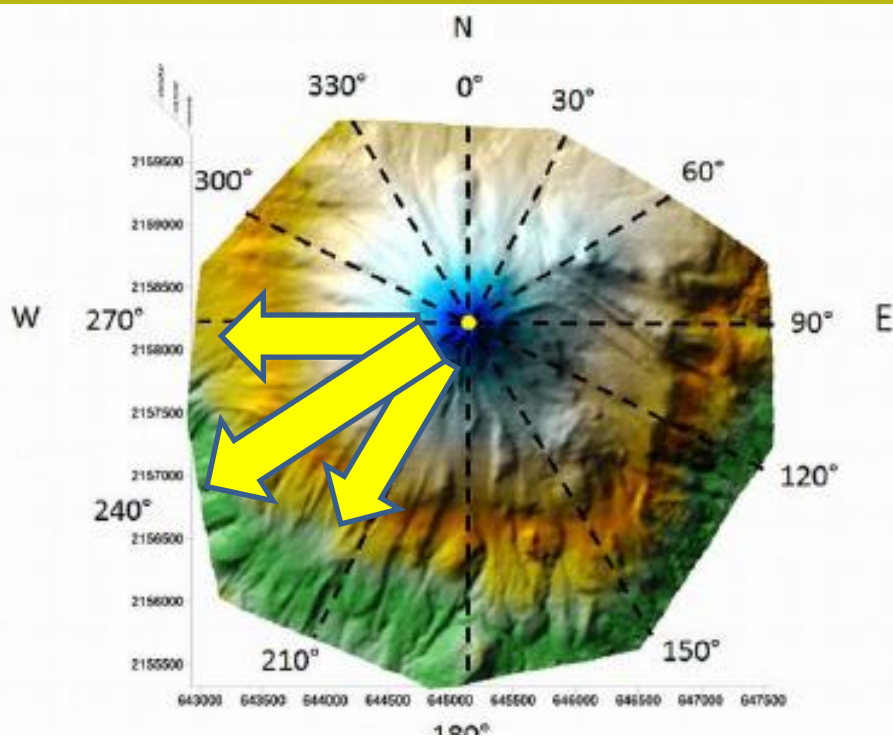
	γ unsaturated unit weight (kN/m^3)	γ_s saturated unit weight (kN/m^3)	σ_1 uniaxial compressive strength of intact rock element (MPa)	GSI geological strength index (adimensional)	m_i lithological index (adimensional)	D disturbance factor (adimensional)
Strato volcano main body	24.5	25.0	50	40, (60)*	22	1.0
Hydrothermal altered body	24.0	24.5	40	30, (45)*	22	1.0
Dome and conduct	24.0	24.5	25	20, (30)*	22	1.0

*In parentheses the GSI value for scenario analysis Nos. 2, 3 and 4 (50% increase assumed with respect to GSI of scenario no. 1).

Characteristics of scenario analysis adopted for limit equilibrium analysis.

Scenario no. 1	Description	Notes
1	Geomechanical parameters as in Table 2	No seismic effect
2	Geomechanical parameters as in Table 2 with GSI increase of 50%	No seismic effect
3	The same as scenario 2, but seismic coefficients $K_h = 0.2$; $K_v = 0.1$	Seismic effect by LEM pseudostatic analysis
4	The same as scenario 2, but seismic coefficient $K_h = 0.25$; $K_v = 0.125$	Seismic effect by LEM pseudostatic analysis





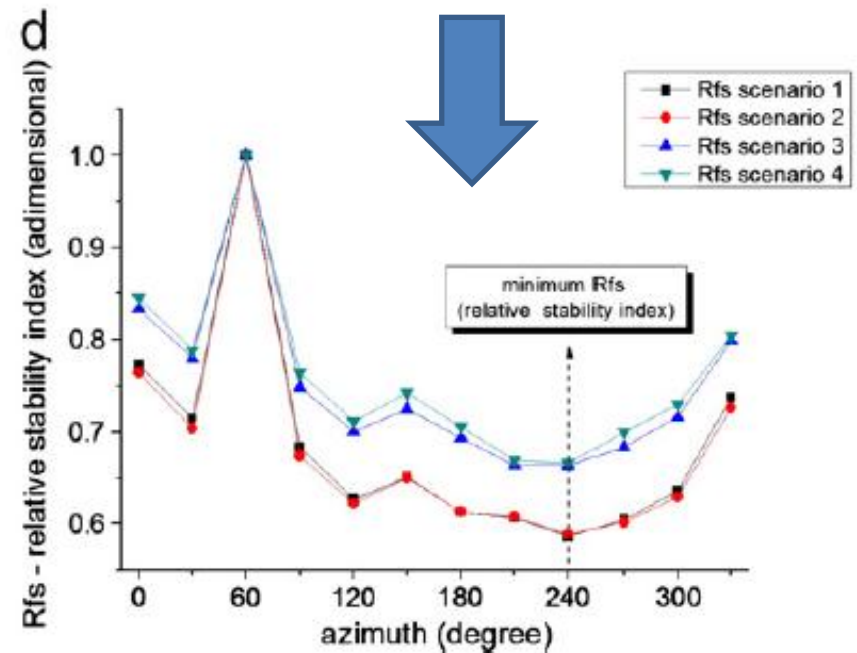
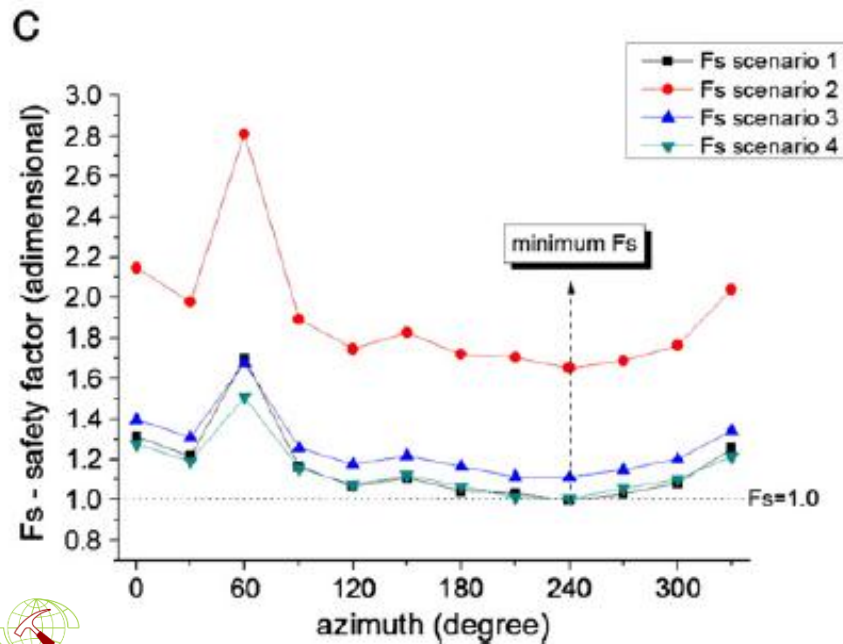
The sector with minimum relative stability is W-SW flank (between 270° and 210°)

The Relative stability index



$$R_{fs_i} = \frac{Fs_i}{Fs_{max}}$$

(Borselli et al. 2011)



$$Z = a e^{-\frac{\sqrt{(x-x_0)^2 + (y-y_0)^2}}{b}} + c \quad \text{if } Z \leq Z_1$$

VOLCANOID SURFACE OF REVOLUTION

ALTERNATIVE VOLCANOID'S GENERATRIX

$$Z = a \cosh\left(\frac{r-c}{b}\right)$$

for $\forall r < c$ and $a, b, c > 0$.

$$Z = \frac{z_1 - a}{1 + e^{\frac{r-c}{b}}}$$

with $z_1 > a$ and $z_1, a, b, c > 0$.

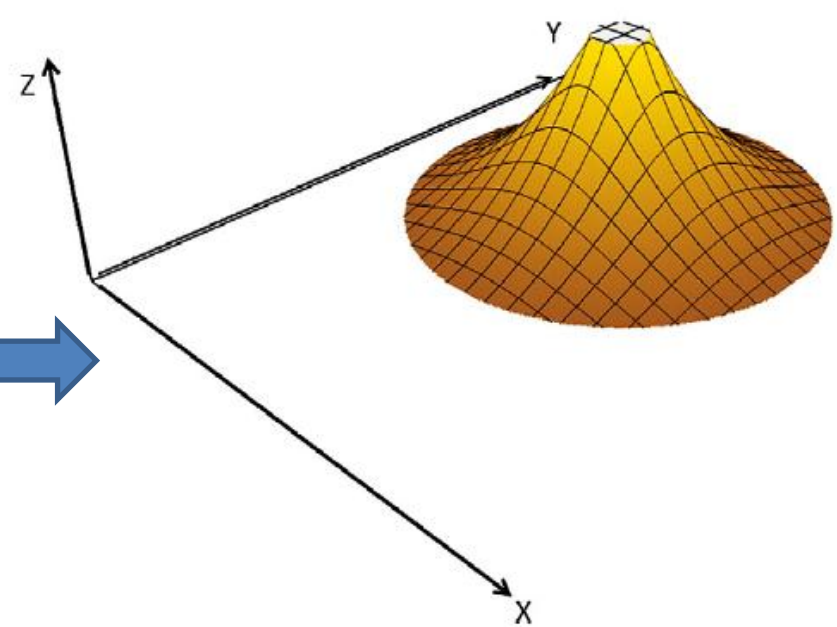


Fig. A.2. Example of volcanoid with constant negative curvature (Eq. (A.5)).

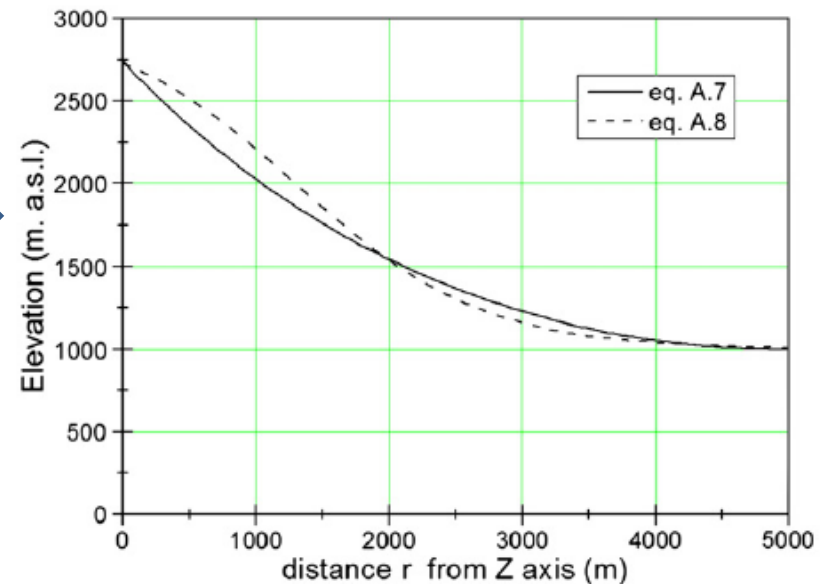


Fig. A.5. Alternative generatrix function of 3D volcanoid.

Colima
Volcanofit 2.0
Result:
Using Negative
exponential
Volcanoid's
generatrix

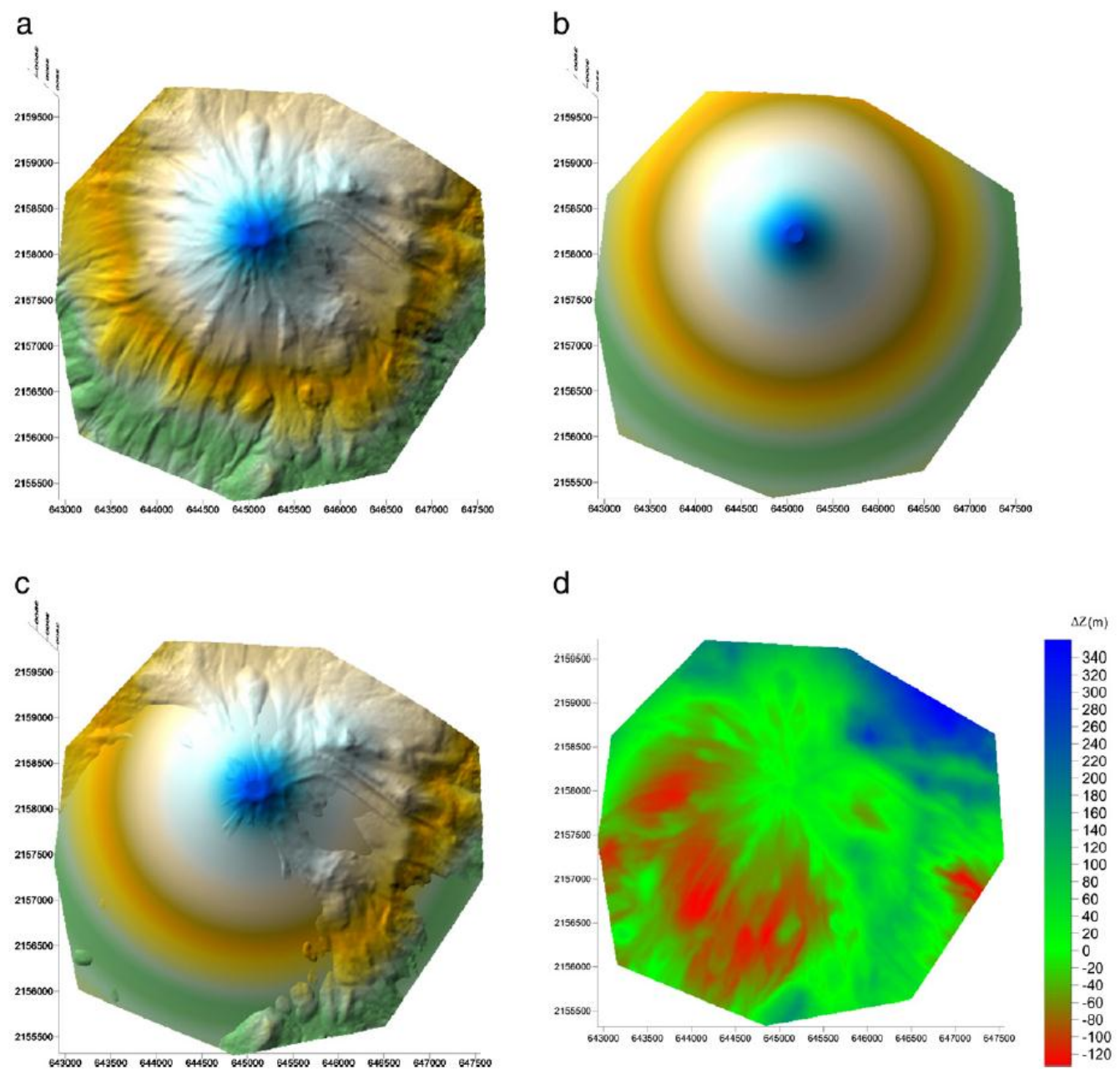
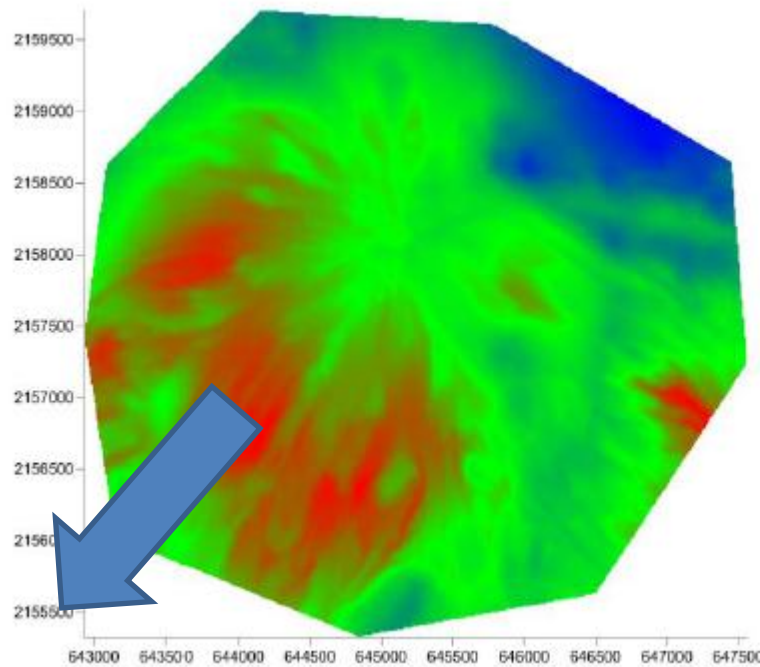
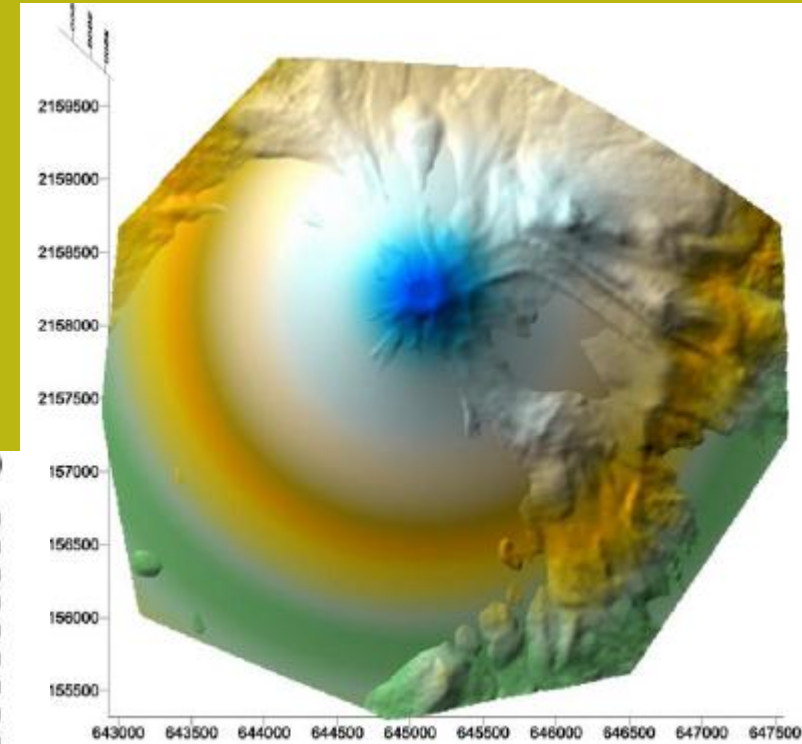
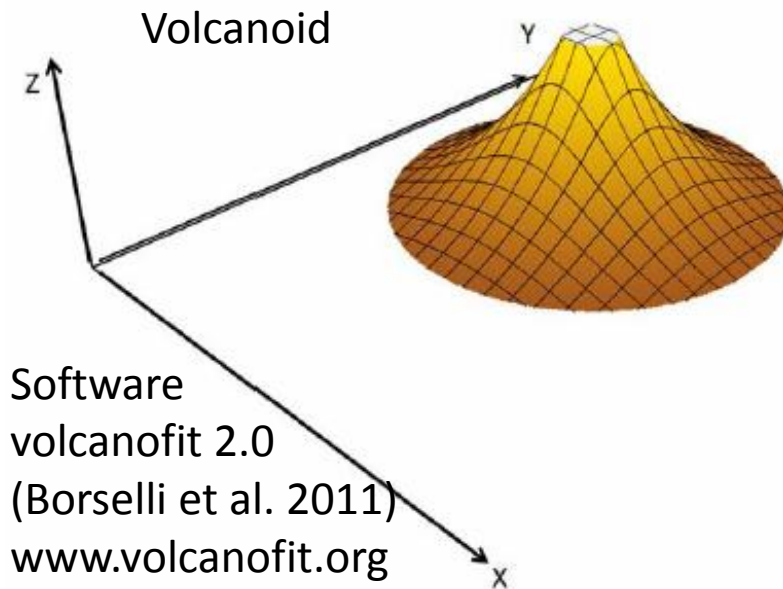
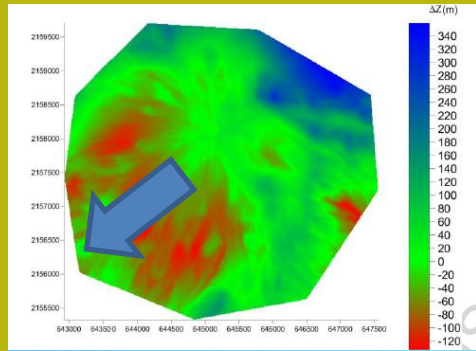


Fig. 7. a) Upper edifice of Colima volcano DEM (2005) b) fitted volcanoid 3D surface Eq. (A.5); c) Upper edifice Colima Volcan de Fuego DEM with overlaid volcanoid Eq. (A.5); d) plot of local deficit (negative values) or surplus (positive values) calculated with Eq. (A.6).

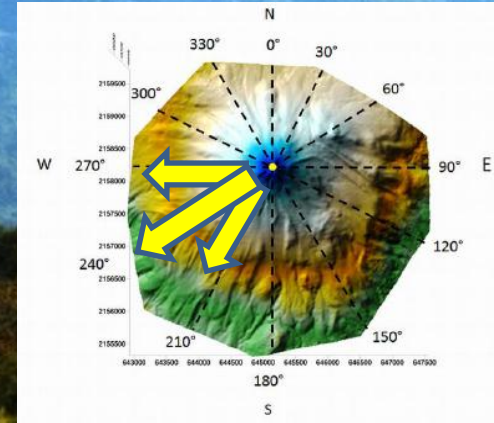
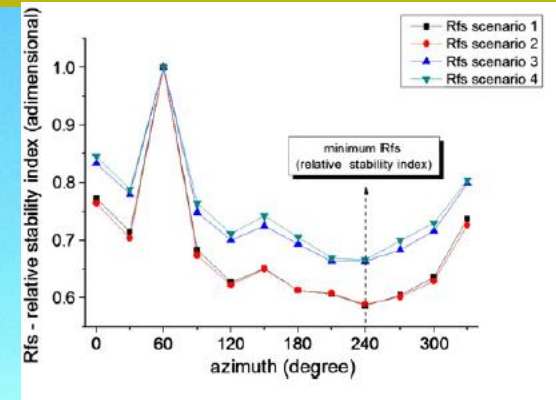
Details overlay DEM and Fitted Volcanoid



Volume (mass) Deficit
in SW flank



The most potentially unstable
Flank: Azimuth 270°-210°



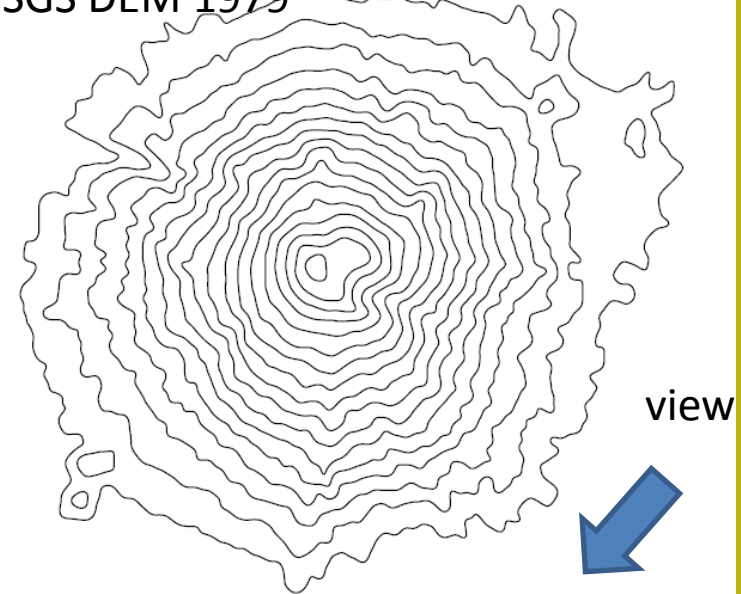
Mt. St. Helens Before 18 may 1980



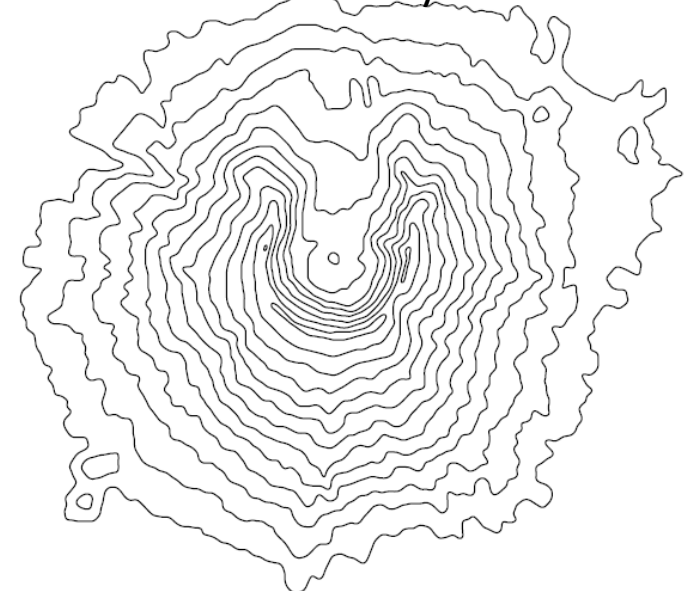
Mt. St. Helens Now



USGS DEM 1979



USGS DEM after 18 may 1980



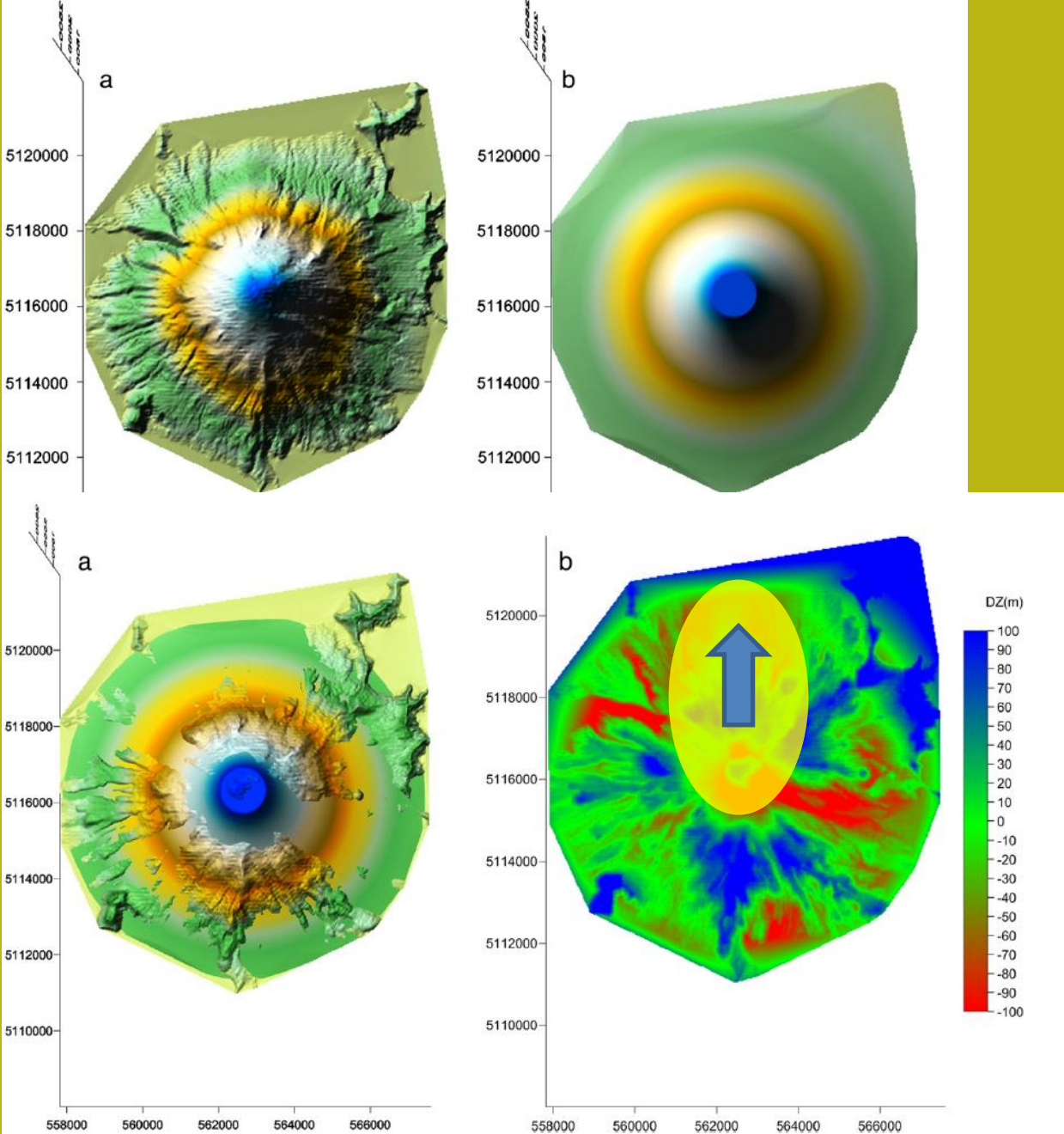
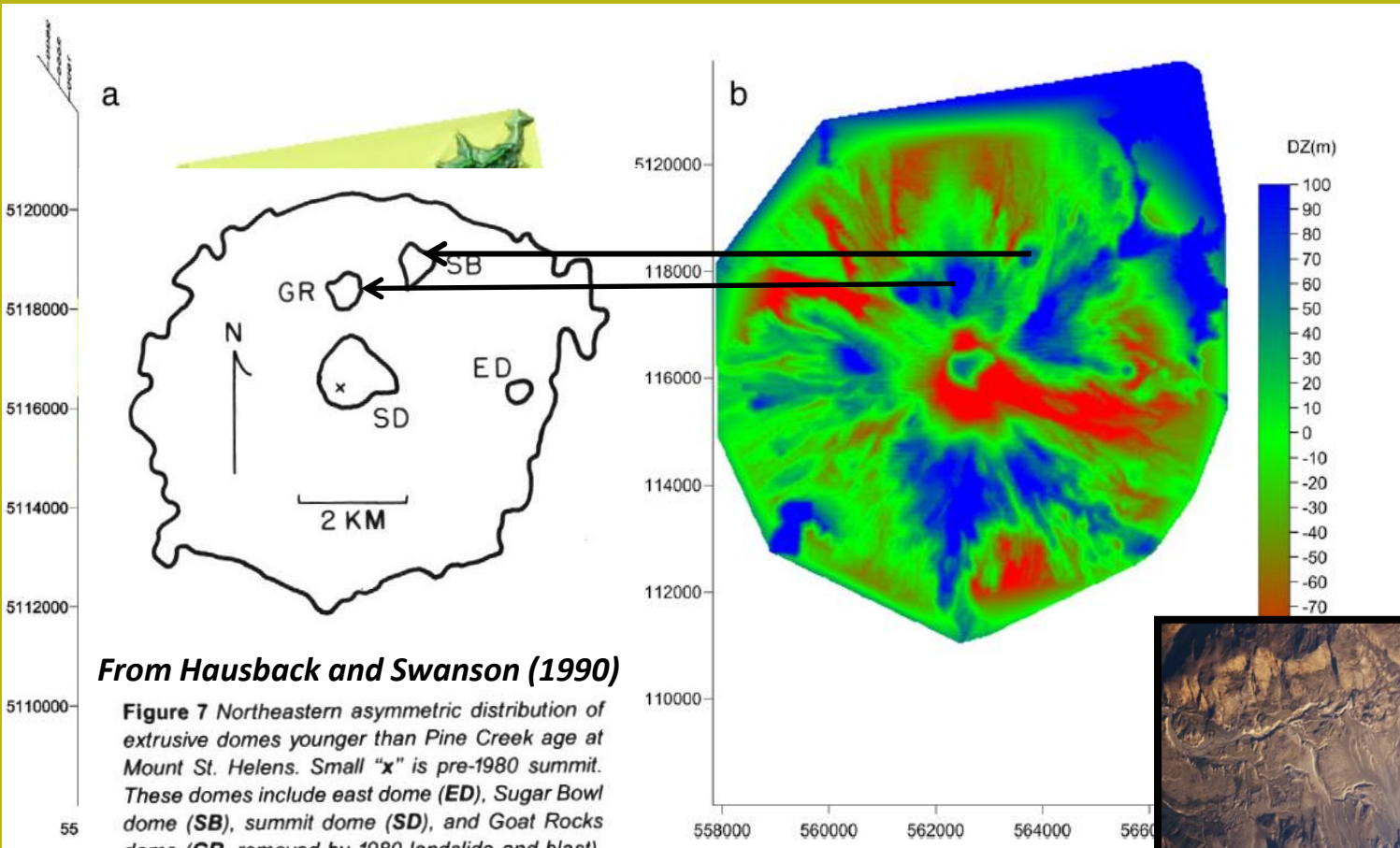


Fig. A.4. a) Pre-eruption 1980 DEM with overlaid volcanoid Eq. (A.5). b) Plot of local deficit (negative values) or surplus (positive values) calculated with Eq. (A.6).



© National Geographic magazine

Mt st. helens 1979 DTM
 Analysed by **VOLCANOFIT 2.0**
 (Borselli et al. 2011)



From Hausback and Swanson (1990)

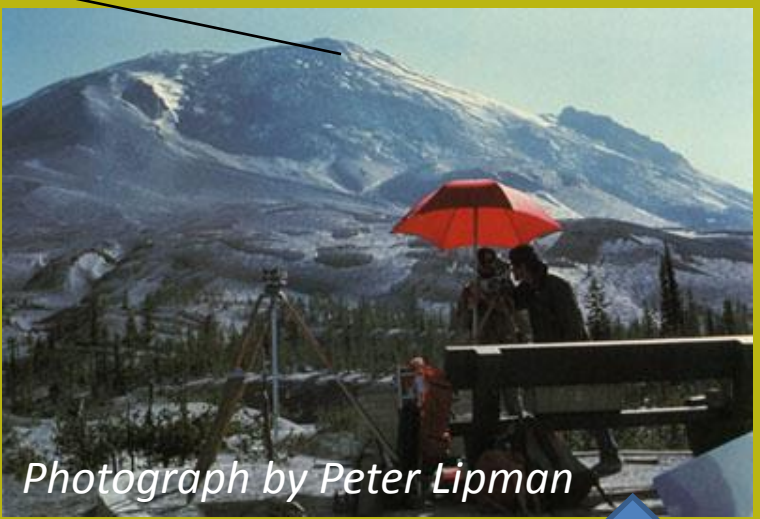
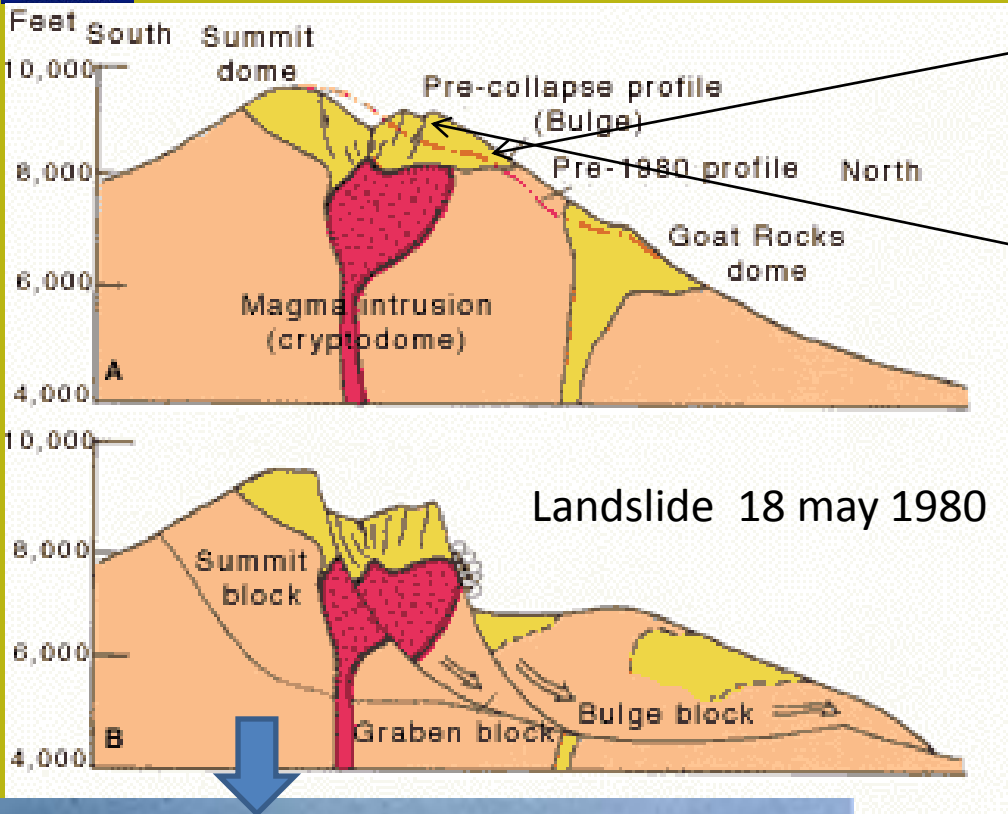
Figure 7 Northeastern asymmetric distribution of extrusive domes younger than Pine Creek age at Mount St. Helens. Small "x" is pre-1980 summit. These domes include east dome (ED), Sugar Bowl dome (SB), summit dome (SD), and Goat Rocks dome (GR, removed by 1980 landslide and blast). The 1340-m (4400-ft) contour encircles volcano. Dome outlines from unpublished mapping by C.A. Hopson.

DTM by University of Washington, Earth and Space science, 2010.
<http://rocky.ess.washington.edu/data/raster/thirtymeter/mtsthelens/OldMtStHelens.zip>



NASA Earth Observatory Image 2009

By (USGS Professional Paper 1250)



View of the "bulge" on the north face of Mount St. Helens, from a measurement site about 2 miles to the northeast 27 April 1980

<http://mountsthelens.com/history-1.html>
http://vulcan.wr.usgs.gov/Volcanoes/MSH/Publications/MSHPPF/MSH_past_present_future.html

Volcan de Colima

time of recurrence of last 5 debris avalanche events (DAE) (Borselli et al. 2011)

Available ages of debris avalanche in the last 10,000 years BP, VEI and calculated intervals between the successive collapses and their corresponding band of uncertainty.

Data source	Event ID Number (-)	VEI* (-)	T_e Debris avalanche events (DAE) (years BP)	ϵT_e Uncertainty on DAE (years)	ΔT_e Interval from previous DAE (years)	$\epsilon \Delta T_e$ Uncertainty on interval from previous DAE (years)
1,2,3	4	5	2580	140	1020	184
2,3	3	5	3600	120	3440	200
2,3	2	6	7040	160	2631	183
2,3	1	5-6	9671	88	3699	149
1,2	0	5-6	13370	120	n.a	n.a
Mean interval of last four DAE (expressed as stochastic number)					ΔT_e Mean interval of last four DAE (years)	$\epsilon \Delta T_e$ Standard deviation associated to mean DAE interval (years)
					2698	180

1 Komorowski et al. (1997); 2 Cortes et al. (2005); 3 Cortes et al., 2010; *from Mendoza-Rosas and De La Cruz-Reyna (2008).

Mean interval of last 4 DAE interval is **2698 years**
with a mean standad deviation of +/- **180 years**

Using stochastic arithmetic
(Vignes, 1993; Markov and Alt, 2004)

USE of Stochastic arithmetic for Debris avalanche recurrence time

The number of DAE is much lower than the number of total explosive events.

De la Cruz-Reyna (1993) established a Poissonian model for the recurrence intervals and occurrence frequency of explosive eruptions, and Mendoza-Rosas and De la Cruz-Reyna (2008, *JVGR* 176, 277–290) analysed the distribution of events **with $VEI > 4$, which may be related to large DAEs, finding an 85% probability of a $VEI > 4$ event within the next 500 yr, and an average recurrence time for $VEI \geq 5$ over 2500 yr. (this analysis include all events $2 < VEI < 6$)**

Instead we use a stochastic arithmetic techniques (Vignes, 1993; Markov and Alt, 2004) adapted to the mean age of DAE and its band of uncertainty. This technique accounts for the error propagation and uncertainty associated with the computation of successive intervals between collapses. The proposed methodology resembles that proposed by Akçiz et al. (2010, *Geology* 38 (9), 787–790) for the assessment of large earthquake recurrence times at the San Andreas Fault (California, st. Andreas Fault system). In this chase the recurrence time for the Big Ones is much more shorter than previous assessments.

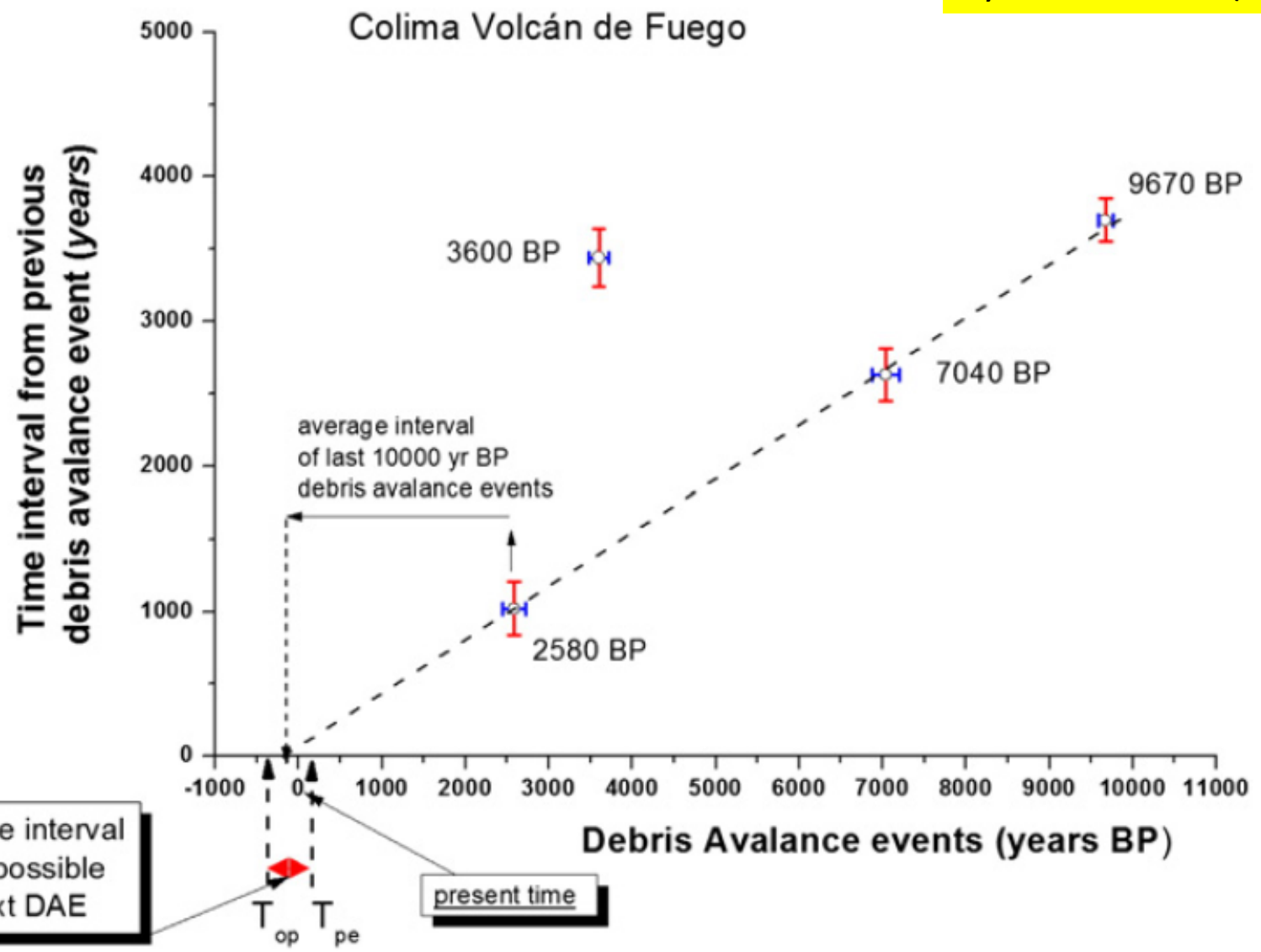


Fig. 6. DAE events vs. time interval from previous debris avalanche event. The projection of a possible scenario for the next DA event is included in the horizontal axis.

Highlights

- **ALEM techniques** applied to Volcán de Colima point to the **W-SW quadrant as potentially the most unstable sector of the edifice** under a wide range of scenarios.
- The VOLCANOFIT application to Colima shows a n important deficit of volume in the same W-SW quadrant (approx. 0.4 km^3).. The VOLCANOFIT Application to Mt. St. Helens pre-eruption 1980 DEM shows the distribution of local mass deficit/surplus association that may be easily correlated with the 1980 incipient flank collapse process. **So there is the possibility that Sector Volume Deficit/Excess anomalies may be correlated to a possible mayor relative instability..**
- The recurrence interval of major collapse events in Colima volcano , during the last 10,000 years, calculated here using a stochastic arithmetic approach, yielding a **mean recurrence interval of 2698 yrs, with an uncertainty range of 180 yrs.**
- Our analysis point out an increased **possibility of flank collapse in the interval between -110 yrs and +345 yrs from the present.** This generates a series of scenarios ranging from **optimistic, considering a collapse within the next 345 years,** to **pessimistic, derived from the 110-year delay.**
- The proposed **new approach may be applied to any stratovolcano with a potential of flank collapse** and for his future hazard assessments.

Gracias por su atención !!!



Many thanks for Your attention !!!